

Online Supplemental Material for:

Schleff EJ, Chmielewski MW, Stark AY and Yanoviak SP. 2026. A comparison of adhesive performance among six cursorial spider species. *The Journal of Arachnology* 53(3):203-207.

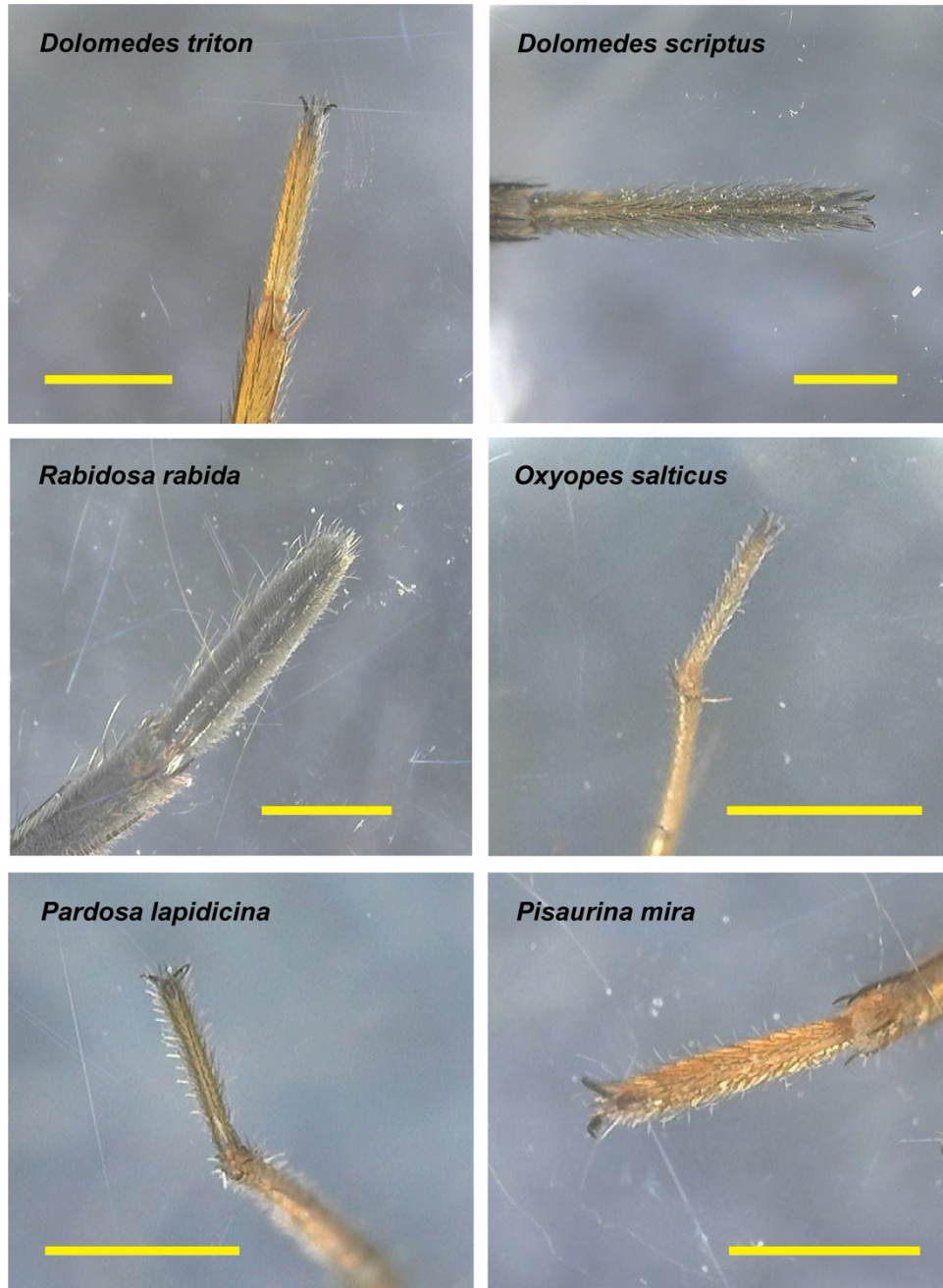


Figure S1.—Images of the second foot (Labarque et al. 2017) of each of the six focal species. Each image is a still frame from a video recording of the spider standing on a glass plate and viewed from beneath. Scale bars = 1.0 mm.



Figure S2.—Image of the second foot of *Pardosa lapidicina* showing the tracing method used to estimate contact area (yellow outline). The image is a still frame from a video recording of the spider standing on a glass plate and viewed from beneath. Scale bar = 1.0 mm.

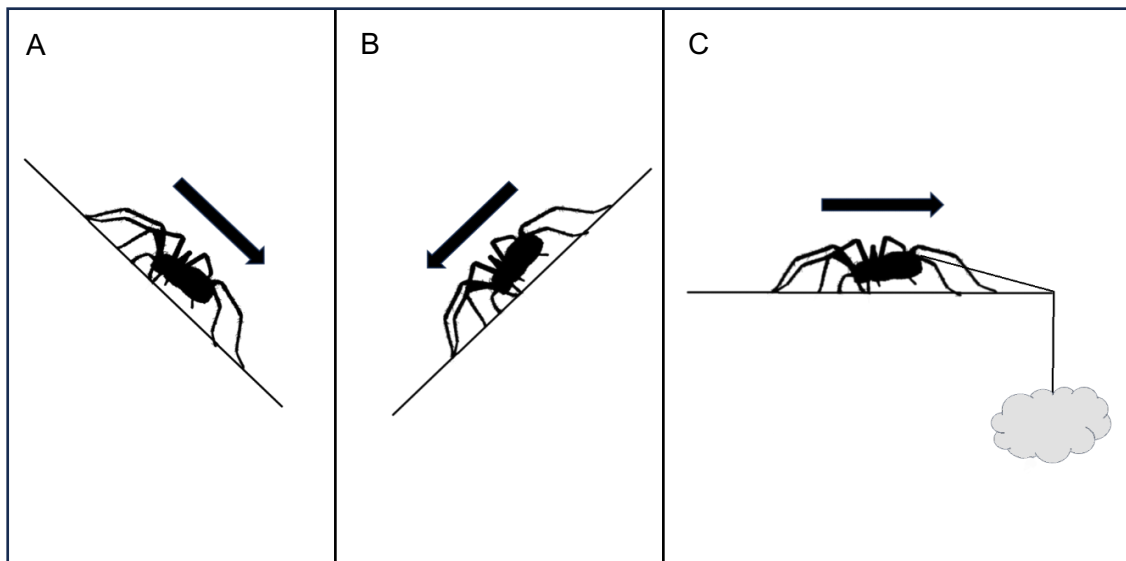


Figure S3.—Diagram of angle of failure tests with the spider facing at an upward angle (A) and downward angle (B). Angle of failure in each case was recorded when the spider slipped down the glass. Shear load tests (C) were conducted by gradually adding water to a cotton ball attached via a nylon thread to the spider's pedicel.

Table S1.—The distribution of individuals among species and sex in the two experiments.

| Species | Angle of Failure | | Shear Load | |
|---------------------------|------------------|--------|------------|--------|
| | Male | Female | Male | Female |
| <i>Dolomedes scriptus</i> | 3 | 11 | 3 | 7 |
| <i>Dolomedes triton</i> | 1 | 9 | 1 | 9 |
| <i>Oxyopes salticus</i> | 9 | 13 | 5 | 9 |
| <i>Pardosa lapidicina</i> | 23 | 19 | 6 | 6 |
| <i>Pisaurina mira</i> | 0 | 7 | 0 | 7 |
| <i>Rabidosia rabida</i> | 6 | 4 | 6 | 4 |

Table S2.—Statistical results for the full model. Shear load data were log-transformed before analysis.

| Response | Predictor | F | df | P |
|--------------------------|--------------------------|--------|-------|--------|
| Shear Load | Sex | < 0.01 | 1, 27 | 0.98 |
| | Tarsal Index | 27.61 | 1, 27 | < 0.01 |
| | Species | 16.44 | 5, 27 | < 0.01 |
| | Species:Tarsal Index | 1.22 | 5, 27 | 0.33 |
| | Species:Sex | 2.86 | 1, 27 | 0.10 |
| | Sex:Tarsal Index | 0.37 | 1, 27 | 0.55 |
| | Species:Sex:Tarsal Index | 1.31 | 1, 27 | 0.26 |
| | Angle of Failure | Sex | 0.21 | 1, 35 |
| Tarsal Index | | 3.35 | 1, 35 | 0.08 |
| Species | | 29.38 | 5, 35 | < 0.01 |
| Species:Tarsal Index | | 1.27 | 5, 27 | 0.30 |
| Species:Sex | | 0.96 | 1, 27 | 0.34 |
| Sex:Tarsal Index | | 0.003 | 1, 27 | 0.96 |
| Species:Sex:Tarsal Index | | 0.82 | 1, 27 | 0.37 |

Table S3.—Medians and ranges [in brackets] for spider parameters and adhesive performance variables measured in the study. PL = *Pardosa lapidicina*, RR = *Rabidosia rabida*, PM = *Pisaurina mira*, DS = *Dolomedes scriptus*, DT = *Dolomedes triton*, and OS = *Oxyopes salticus*. * = mean \pm SE shown in Figure 1 of the main text. Within *Shear Load* and *Failure Angle* columns, similar letters indicate means (from Figure 1) that do not differ based on Tukey post-hoc tests.

| Species | Mass* (mg) | Tarsal index ($\mu\text{m}^2 \text{mg}^{-1}$) | Shear load* (g) | Failure Angle* ($^\circ$) |
|---------|------------------------|--|-------------------------|--------------------------------|
| DS | 308.1 [16.8-1115.6] | 157.7 [81.4-283.7] | 0.37 cd [0.06-0.52] | 44.7 a [29.7-65.1] |
| DT | 110.8 [27-393.9] | 145.8 [103.7-175.9] | 0.20 bcd [0.06-0.84] | 50.2 a [40.1-64.8] |
| OS | 12.0 [3.7-23.9] | 99.7 [81.6-144.4] | 0.03 a [0.01-0.08] | 46.9 a [35.4-61.3] |
| PL | 31.2 [7.5-115.2] | 133.7 [51.1-217.3] | 0.05 ab [0.01-0.67] | 46.8 a [33.9-65.0] |
| PM | 46.8 [17.7-117.8] | 147.9 [99.0-248.4] | 0.08 abc [0.04-0.23] | 46.0 a [38.4-54.4] |
| RR | 192.7 [116.1-280.5] | 101.3 [90.5-133.8] | 0.37 d [0.15-0.74] | 61.4 b [50.2-70.3] |

Table S4.—Species-specific regression results for shear load and angle of failure vs. tarsal index. PL = *Pardosa lapidicina*, RR = *Rabidosia rabida*, PM = *Pisaurina mira*, DS = *Dolomedes scriptus*, DT = *Dolomedes triton*, and OS = *Oxyopes salticus*.

| Predictor | Species | R ² | F | df | P |
|------------------|---------|----------------|------|-----|------|
| Shear Load | DS | 0.53 | 340 | 1,3 | 0.16 |
| | DT | 0.68 | 8.31 | 1,4 | 0.05 |
| | OS | 0.36 | 1.70 | 1,3 | 0.28 |
| | PL | 0.50 | 7.92 | 1,8 | 0.02 |
| | PM | 0.42 | 3.56 | 1,5 | 0.12 |
| | RR | 0.01 | 0.08 | 1,8 | 0.78 |
| Angle of Failure | DS | 0.11 | 0.39 | 1,3 | 0.58 |
| | DT | 0.32 | 1.89 | 1,4 | 0.24 |
| | OS | 0.01 | 0.03 | 1,3 | 0.87 |
| | PL | 0.35 | 4.40 | 1,8 | 0.07 |
| | PM | 0.04 | 0.23 | 1,5 | 0.65 |
| | RR | 0.38 | 4.88 | 1,8 | 0.06 |